



RESEARCH ARTICLE | FEBRUARY 22 2024

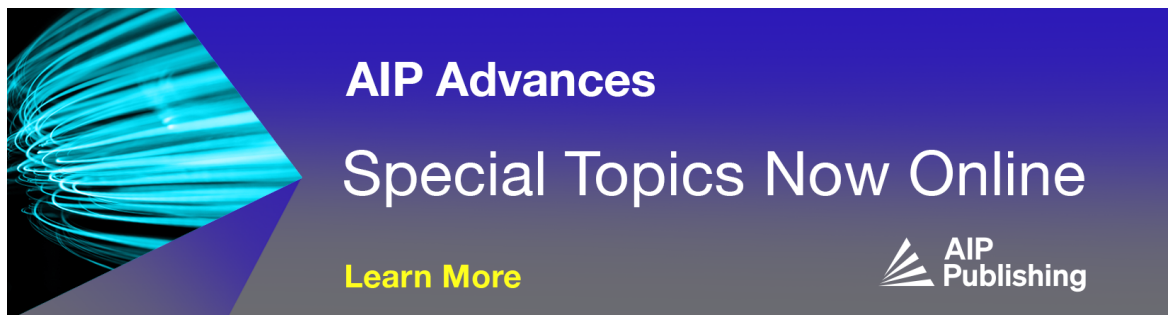
Modeling Fermi energy, free-carrier density, and resistivity in degenerate n-Ge

Luigi Abenante  




AIP Advances 14, 025141 (2024)

<https://doi.org/10.1063/5.0163730>



AIP Advances
Special Topics Now Online

[Learn More](#)



Modeling Fermi energy, free-carrier density, and resistivity in degenerate n-Ge

Cite as: AIP Advances 14, 025141 (2024); doi: 10.1063/5.0163730

Submitted: 21 June 2023 • Accepted: 25 January 2024 •

Published Online: 22 February 2024



Luigi Abenante^{a)}

AFFILIATIONS

ENEA, Italian National Agency for New Technologies, Energy and Sustainable Economic Development, Roma, Italy

^{a)} Author to whom correspondence should be addressed: clovocloodo@gmail.com

ABSTRACT

A new expression for Fermi energy vs doping is derived using the standard model for free carriers in n-type semiconductors. The new expression is composed of the Fermi energy in non-degenerate semiconductors, a doping function for bandgap narrowing (*BGN*), and an adjustable energy variation. In non-degenerate semiconductors, the new expression is equivalent to the standard Boltzmann expression. Calculated curves of Fermi energy are assigned in the Fermi–Dirac expression for the donor ionization ratio, and reported data of electron density and resistivity measured in heavily doped n-Ge layers are fitted. Five reported doping functions for *BGN* are used. One of the *BGN* functions allows modeling frustrated incomplete ionization. Another allows modeling bandgap widening.

© 2024 Author(s). All article content, except where otherwise noted, is licensed under a Creative Commons Attribution (CC BY) license (<http://creativecommons.org/licenses/by/4.0/>). <https://doi.org/10.1063/5.0163730>

I. INTRODUCTION

Availability of curves of free-carrier density, n , as a function of variables, such as doping density, N , temperature, and energy, is a precondition for the modeling and simulation of semiconductor devices. A standard model to calculate n as a function of N has been derived by combining Fermi–Dirac (FD) and Boltzmann (B) statistics.^{1,2} In particular, the curve of Fermi energy, E_F , calculated at B statistics is substituted in the FD expression for the donor ionization ratio, n/N . In electronics, n-Ge layers are used,^{3–7} where $n \approx N$ is measured^{4–6} at high doping values ($N > 10^{18} \text{ cm}^{-3}$). In highly doped semiconductors, the standard model calculates $n \ll N$ (Refs. 8–10). In these cases, full ionization ($n = N$) is imposed at any N -value² or the standard model is parameterized such that incomplete ionization is frustrated at dopings higher than the Mott concentration.^{4,8–10} The latter approach reduces to the former at high dopings.

In the present work, we show that the standard model fails in calculating n in heavily doped semiconductors because it neglects heavy-doping effects. We calculate, in fact, $n(N)$ -curves that agree with measurements at all dopings by assigning a new expression to E_F , where bandgap narrowing (*BGN*) is included together with a variation of conduction band, ΔE_C . The new expression is derived by exploiting the standard model. *BGN* is commonly used to model heavy-doping effects.^{12–15} We assume $\Delta E_C = \text{BGN}$ in non-degenerate semiconductors and $\Delta E_C \neq \text{BGN}$ in degenerate

semiconductors. In the latter case, *BGN* is assigned an N -function and ΔE_C is considered as an adjustable parameter independent of N . Data of n and resistivity measured in five reported sets of n-Ge layers^{4–7,11} are fitted. Five reported doping functions for *BGN*^{12–15} are used. One of the *BGN* functions¹⁵ provides $n(N)$ -curves that simulate frustrated incomplete ionization⁴ at high dopings. Another¹³ allows detecting possible bandgap widening in Sb:Ge and a set of P:Si layers.⁷ In the new model for $E_F(N)$, the standard $E_F(N)$ -curve is included. Calculating the standard $n(N)$ -curve in non-degenerate n-Ge is consequently necessary. In this work, a calculation approach is adopted, where n is a fraction of active dopant density.¹⁰

II. DERIVATION

Free-carrier density, n , in n-Ge can be calculated with the Fermi–Dirac (FD) expression for the ionization ratio, n/N , in n-type semiconductors,

$$\frac{n}{N} = 1 - \frac{1}{1 + g \exp[(E_D - E_F)/kT]}, \quad (1)$$

where g is the degeneracy factor, E_D is the dopant energy, k is the Boltzmann constant, and T is the temperature. With N_C being the effective density of states in the conduction band and E_C being

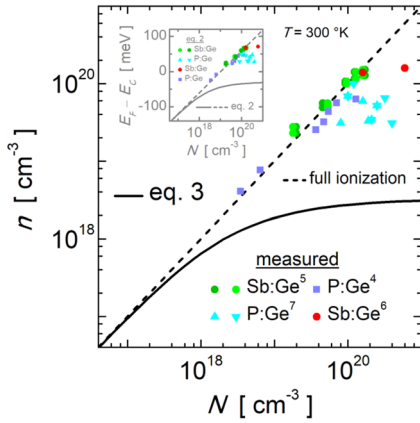


FIG. 1. The standard $n(N)$ -curve for n-Ge (black full line) calculated with (3) according to Ref. 10. Experimental data (symbols), $n(N)$ -curves at full ionization, and standard curves of $E_F - E_C$ vs N calculated with (2) are also shown.

the energy at the bottom of the conduction band, substituting the Boltzmann (B) expression for Fermi energy, E_F ,

$$E_F = kT \ln\left(\frac{n}{N_C}\right) + E_C, \quad (2)$$

in (1) yields

$$\frac{n}{N} = 1 - \frac{n}{n + gN_C \exp[(E_D - E_C)/kT]}, \quad (3)$$

which is the aforementioned standard model for n in n-type semiconductors. The standard $n(N)$ -curve calculated in n-Ge at $N_C = 1.04 \times 10^{19} \text{ cm}^{-3}$ and $E_D = -12 \text{ meV}$ with (3) according to Ref. 10 is shown in Fig. 1 with a black full line together with experimental data (symbols), $n(N)$ -curves at full ionization (dashed lines), and standard curves of $E_F - E_C$ vs N calculated with (2) using calculated and measured values of n . As can be seen, at high dopings, (3) calculates $n \ll N$.^{4,8-10} As aforementioned, $n \approx N$ can be obtained by imposing full ionization at all dopings or reducing the occupation probability of E_D in (3) at dopings higher than the Mott concentration,^{4,8-10} which is equivalent to imposing frustrated incomplete ionization.⁴ The latter approach converges to the former at heavy dopings.

At heavy dopings, heavy-doping effects may prevent full ionization. Heavy doping effects are usually modeled with functions for bandgap narrowing, BGN .¹²⁻¹⁵ BGN is defined as $BGN = E_{C,0} - E_C$, with $E_{C,0}$ being a reference energy. Adding and subtracting $E_{C,0}$ in (2) gives

$$E_F = -BGN + kT \ln\left(\frac{n}{N_C}\right) + E_{C,0}. \quad (4)$$

$E_{C,0}$ can be written as $E_{C,0} = E_C + \Delta E_C$, where ΔE_C is a variation of E_C . We obtain

$$E_F = -BGN + \Delta E_C + E_C + kT \ln\left(\frac{n}{N_C}\right), \quad (5)$$

where (2) is included. Equation (5) is the new expression for $E_F(N)$ presented in this work. We assume that (5) is rigorously equivalent

to (2) in non-degenerate semiconductors. Non-degenerate semiconductors can be so defined as semiconductors, where $BGN = \Delta E_C$. The remaining semiconductors are degenerate. In this case, both BGN and ΔE_C can be used as adjustable parameters or can be assigned a doping function. Nothing prevents BGN and ΔE_C in (5) from being assigned negative values. Due to the definition of BGN , assigning a negative value to BGN is equivalent to assigning bandgap widening.

III. APPLICATION

The following $BGN(N)$ -functions for n-Ge are assigned in (5):

The linear function:¹² $BGN = 0.013 + 10^{21} \times N$.

The minimum function:¹² $BGN = 8.15 \times (N/10^{18})^{1/4} + 2.03 \times (N/10^{18})^{1/2}$.

The function of Jain and Roulston [Eq. (12), Ref. 13]:

$$BGN = R \left[\frac{1.83}{r_s} \frac{\Lambda}{N_b^{1/3}} + \frac{0.95}{r_s^{3/4}} + \frac{1.57}{N_b r_s^{3/2}} \left(1 + \frac{R_{min}}{R} \right) \right], \quad (6)$$

where $N_b = 4$, $\Lambda = 0.84$, $R = 12.6 \text{ meV}$, $R_{min} = 11.2 \text{ meV}$, and $r_s = [3/(4\pi N)]^{1/3}/37.1 \times 10^{-8}$.

The function of Xu *et al.*:¹⁴ $BGN = 16(N/10^{19})^{0.66}$.

The function of Van Cong:¹⁵

$$BGN = 20.995 \times \left\{ \left[N - \frac{3}{4\pi} \left(\frac{3\xi^2 kT}{2E_x a_x} \right)^{3/2} + n_i \right] / 10^{18} \right\}^{0.2998}, \quad (7)$$

where $\xi = N/N_C$, $E_x = 2.65 \text{ meV}$, the intrinsic concentration in Ge $n_i = 10^{13} \text{ cm}^{-3}$, and $a_x = 177 \times 10^{-8} \text{ cm}$. The five BGN functions are graphed in Fig. 2.

Four sets of $n(N)$ -data measured in highly doped P:Ge^{4,7} and Sb:Ge^{5,6} are shown in Figs. 1, 4, and 5 with symbols. The values in Sb:Ge from Ref. 5 (light and dark green circles) are relevant to two different measurements of N . The values in P:Ge from Ref. 7 (cyan triangles) are relevant to two sets of samples. The shown $n(N)$ -data are measured with infrared spectroscopic ellipsometry.⁷ The values of Sb:Ge from Ref. 6 (red circles) are relevant to two samples, in one of which n depends on the film thickness. The maximum n -value is attributed to this sample. Experimental values of $E_F - E_C$

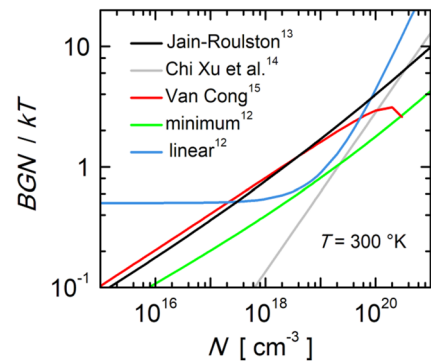


FIG. 2. The five BGN -functions used in the present work.

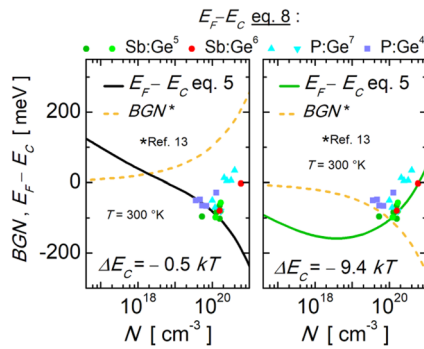


FIG. 3. Curves of $E_F - E_C$ vs N calculated in this work with (5) (black and green lines) are shown together with the used BGN functions¹³ (dashed lines) and experimental values calculated with (8) (symbols) using measured $n(N)$ -values.

vs N can be obtained by assigning the measured values of N and n in the expression for E_F implied by (1),

$$E_F = E_D - kT \ln \left[\frac{1}{g} \left(\frac{n}{N - n} \right) \right]. \quad (8)$$

The five functions plotted in Fig. 2 are assigned to BGN in (5), and (5) is assigned in (1) to fit at 300 °K the aforementioned four sets of n data by adjusting ΔE_C . The curve of $E_F - E_C$ vs N calculated with (5) using the BGN function of Jain and Roulston¹³ is shown in Fig. 3 (full black line) together with experimental values of $E_F - E_C$ vs N calculated with (8) (symbols), the curve of BGN (dashed line), and the fit-value of ΔE_C . Calculated $n(N)$ -curves (lines) are shown in Fig. 4 together with the n data (symbols) and the fit-values of ΔE_C .

A curve of $E_F - E_C$ vs N calculated with (5), where the BGN function of Jain and Roulston¹³ is assigned negative sign, is shown

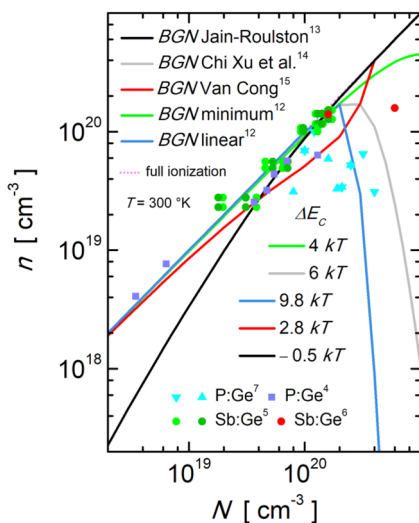


FIG. 4. Measured data of n in n-Ge (symbols) and fit-curves (lines) calculated with (1) using (5) to calculate Fermi energy. The BGN -functions⁴⁻⁷ in Fig. 2 are assigned to BGN in (5). The listed values are assigned to ΔE_C .

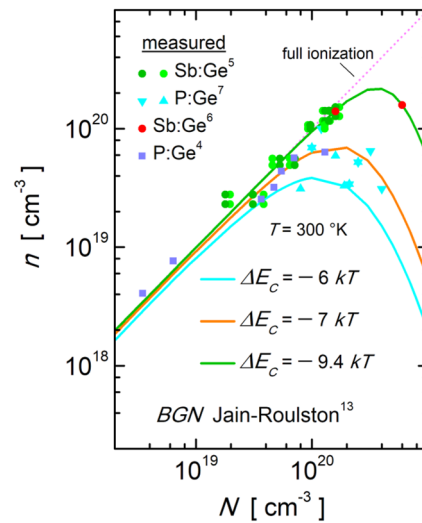


FIG. 5. $n(N)$ -data measured in n-Ge layers (symbols) and fit-curves (lines) calculated with (1) using model (5) for Fermi energy, where BGN is assigned the Jain-Roulston BGN -function¹³ with negative sign.

in Fig. 3 together with the experimental values of $E_F - E_C$ vs N (symbols), the curve of BGN (dashed line), and the fit-value of ΔE_C . Using this curve in (1) gives the green-line $n(N)$ -curve shown in Fig. 5, which fits Sb:Ge data from Refs. 5 and 6. The remaining n -data in Fig. 5 are fitted by two $n(N)$ -curves (orange and cyan lines) calculated with the negative Jain-Roulston¹³ function at different ΔE_C -values.

IV. DISCUSSION

In the application of model (5), ΔE_C has been considered as an adjustable parameter. This is because BGN -functions give, in general, negligible values at low dopings so that E_F in this case tends to a constant value and (1) tends to a straight line, modeling full ionization at low dopings.

Based on a reported parameterization of (3),^{4,8,9} frustrated incomplete ionization has been predicted⁴ in n-Ge layers at $N > 2.6 \times 10^{17} \text{ cm}^{-3}$, which is the Mott concentration in n-Ge. Frustrated incomplete ionization can be simulated with the model presented in this work by assigning the Van Cong¹⁵ function (7) to BGN in (5), as can be seen in Fig. 4 (red line).

Comparing the curves of $E_F - E_C$ vs N and $n(N)$ calculated with the Jain-Roulston¹⁵ function for BGN with positive and negative sign, which are reported in Figs. 3–5, leads to the conclusion that, in the case of the Jain-Roulston BGN function, the two modeling approaches are comparable in terms of fitting capability. In particular, the data in P:Ge from Ref. 7 (Cyan triangles), which are very scattered, and the two data in Sb:Ge from Ref. 6 (red circles) can only be fitted with a single curve using the negative BGN -function (green line), as can be seen in Figs. 3 and 5. Most of the data from Refs. 4 and 5 are instead fitted using the positive BGN -function (black line), as can be seen in Figs. 3 and 4. A further comparison can be made

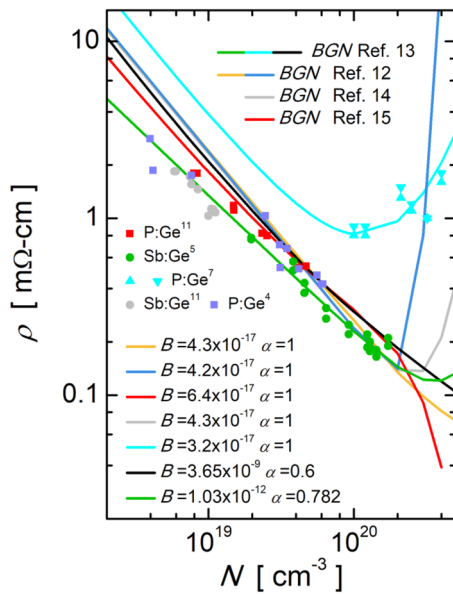


FIG. 6. Measured $\rho(N)$ -data^{4,5,7,11} (symbols) and $\rho(n)$ -curves obtained by assigning calculated $n(N)$ -curves in the empirical expression for ρ of Cuttriss.¹⁶ Assignments to the Cuttriss parameters and BGN are reported.

by assigning the calculated $n(N)$ -curves in the Cuttriss¹⁶ empirical expression for resistivity, $\rho(n)$,

$$\rho = n^{-\alpha}/B, \quad (9)$$

where α and B are adjustable parameters. All the $n(N)$ -curves in Fig. 4 and two $n(N)$ -curves in Fig. 5 (green and cyan lines) are assigned in (9). Results are shown in Fig. 6 (lines), where they are compared to measured values^{4,5,7,11} (symbols). As can be seen, all BGN functions allow fitting measured data to some extent. In particular, the curves calculated using the BGN-function of Jain–Roulston with negative sign (green and cyan lines). The $\rho(n)$ -data from Ref. 7 (cyan triangles) can only be fitted by using one of these $n(N)$ -curves (cyan line— $\Delta E_C = -6$ kT). The other of these $\rho(n)$ -curves (green line— $\Delta E_C = -9.4$ kT) fits accurately nearly all the $\rho(n)$ -data in Sb:Ge. As aforementioned, the corresponding $n(N)$ -curve in Fig. 5 (green line) fits nearly all the $n(N)$ -data measured in Sb:Ge. We conclude that in the set of P:Ge layers from Ref. 7 and in Sb:Ge, bandgap widening is to be expected.

From the fits in Fig. 6, one can observe a reverse dependence of ρ on n . This dependence has not been observed before due to the lack of continuous $n(N)$ -functions, such as those calculated in this work. Cuttriss¹⁶ did not use a continuous single function to fit the data with (9) but rather successive contiguous functions of N with different assignments to α and B in different doping ranges.

V. CONCLUSIONS

A new expression for Fermi energy vs doping, where heavy doping effects are considered, has been derived in this work from

the standard model for free carriers in n-type semiconductors. Curves of Fermi energy vs doping calculated with the new expression have been assigned in the Fermi–Dirac expression for the donor ionization ratio, and data of electron density and resistivity measured in highly doped n-Ge, which cannot be fitted with previous models, have been fitted. The new approach to calculate the Fermi energy and free-carrier density in n-Ge is then free from the limitations affecting previous approaches. Such limitations are due to the fact that previous models do not consider heavy-doping effects. Thanks to one of the five reported functions for bandgap narrowing that have been used in this work, the new expression can model frustrated incomplete ionization at high dopings. Thanks to another reported bandgap narrowing function, it can detect bandgap widening.

AUTHOR DECLARATIONS

Conflict of Interest

The author has no conflicts to disclose.

Author Contributions

Luigi Abenante: Conceptualization (equal); Data curation (equal).

DATA AVAILABILITY

The data that support the findings of this study are available from the corresponding author upon reasonable request.

REFERENCES

- W. Shockley, *Electrons and Holes in Semiconductors* (Van Nostrand, New York, 1950), p. 233.
- K. Wolfstirn, *J. Phys. Chem. Solids* **16**, 279 (1960).
- J. K. Kennedy and W. D. Potter, *J. Cryst. Growth* **13–14**, 315 (1972).
- C. Xu, C. L. Senaratne, J. Kouvetakis, and J. Menendez, *Appl. Phys. Lett.* **105**, 232103 (2014).
- C. Xu, C. L. Senaratne, P. Sims, J. Kouvetakis, and J. Menéndez, *ACS Appl. Mater. Interfaces* **8**(36), 23810 (2016).
- M. Oehme, J. Werner, and E. Kasper, *J. Cryst. Growth* **310**, 4531 (2008).
- G. D. Dilliway, R. van den Boom, A. Moussa, F. E. Leys, B. Van Daele, B. Parmentier, T. Clarysse, E. R. Simoen, C. Defranoux, M. M. Meuris, A. Benedetti, O. Richard, and H. Bender, *ECS Trans.* **3**(7), 599 (2006).
- P. P. Altermatt, A. Schenk, and G. Heiser, *J. Appl. Phys.* **100**, 113714 (2006).
- P. P. Altermatt, A. Schenk, B. Schmithüsen, and G. Heiser, *J. Appl. Phys.* **100**, 113715 (2006).
- L. Abenante, *AIP Adv.* **13**, 015109 (2023).
- W. G. Spitzer, F. A. Trumbore, and R. A. Logan, *J. Appl. Phys.* **32**, 1822 (1961).
- S. C. Jain and D. J. Roulston, *Solid-State Electron.* **34**(5), 453 (1991).
- R. Camacho-Aguilera, Z. Han, Y. Cai, L. C. Kimerling, and J. Michel, *Appl. Phys. Lett.* **102**, 152106 (2013).
- C. Xu, J. Kouvetakis, and J. Menéndez, *J. Appl. Phys.* **125**(8), 085704 (2019).
- H. Van Cong, *Phys. B* **405**, 1139–1149 (2010).
- D. B. Cuttriss, *Bell Syst. Tech. J.* **40**(2), 509 (1961).